

A Red Flag Threat Index Based on the Real-Time Mesoscale Analysis for Use in the Warn-on-Forecast System

Thomas A. Jones,^{a,b,c} T. Todd Lindley,^d Patrick Skinner,^{a,b,c} and Ryan R. Barnes^e

KEYWORDS:

Wildfires;
Numerical weather prediction/
forecasting;
Operational forecasting;
Short-range prediction;
Decision support

ABSTRACT: The increasing frequency of high-impact wildfires has led to an emphasis on improving forecasts of the conditions that are favorable for wildfire initiation and rapid spread. The key atmospheric forecast products currently used are derived from low-level humidity and wind speed. One product that has seen widespread use by the National Weather Service (NWS) in the southern plains is known as the red flag threat index (RFTI). RFTI represents an index ranging from 0 to 10 where larger values indicate a more critical threat for favorable wildfire conditions. The current RFTI is based on 2-m humidity and 6-m wind speed climatologies from surface measurement sites located within a NWS forecast area resulting in a product that differs somewhat from office to office. RFTI forecasts are also only available from existing numerical weather prediction systems such as the Texas Tech modeling system that do not output forecasts with the temporal resolution and latency to forecast rapidly evolving environmental conditions. To address these limitations, this work describes the creation of a grid-based RFTI using a 5-yr, high-resolution (3-km, hourly) reanalysis product known as the Real-Time Mesoscale Analysis (RTMA). Using RTMA data allows for continuous wind and humidity climatology fields to be developed for a larger W-CONUS domain, potentially expanding the use of RFTI. We combine these new climatologies with forecast output from the Warn-on-Forecast System (WoFS) which provides short-term (0–6 h) probabilistic forecasts of high-impact weather over a regional domain. RFTI forecasts from examples occurring in 2022 and 2024 will be discussed as well as its evaluation in the new Fire Weather Testbed.

DOI: 10.1175/BAMS-D-24-0028.1

Corresponding author: Thomas A. Jones, thomas.jones@noaa.gov

Manuscript received 6 February 2024, in final form 30 October 2024, accepted 8 November 2024

© 2024 American Meteorological Society. This published article is licensed under the terms of the default AMS reuse license. For information regarding reuse of this content and general copyright information, consult the AMS Copyright Policy (www.ametsoc.org/PUBSReuseLicenses).

AFFILIATIONS: ^a Cooperative Institute for Severe and High-Impact Weather Research and Operations, University of Oklahoma, Norman, Oklahoma; ^b NOAA/National Severe Storms Laboratory, Norman, Oklahoma; ^c School of Meteorology, University of Oklahoma, Norman, Oklahoma; ^d NOAA/National Weather Service, Norman, Oklahoma; ^e NOAA/NWS/NCEP, Storm Prediction Center, Norman, Oklahoma

1. Introduction

Destructive wildland fires represent a significant threat to human life and property and have been rapidly increasing in frequency owing to a combination of land surface modification, population increases in fire prone regions, and the impacts of climate change (e.g., Peace et al. 2020). All these factors are particularly relevant in the central and western United States where many high-impact wildfires such as the Camp Fire (2018) in California, the Marshall Fire in Colorado (2021), and the Smokehouse Creek Fire (2024) in north Texas have occurred in recent years (Chow et al. 2022; Troy et al. 2022). The key parameters are atmospheric moisture content, wind speed, land surface conditions, and fuel types (e.g., Parks et al. 2014). The first two are forecast by numerical weather prediction (NWP) models, but most operational forecast models do not output these parameters with the spatial or temporal resolution necessary to fully capture rapidly changing (subhourly) conditions. Convection-allowing models (CAMs) such as the operational High-Resolution Rapid Refresh (HRRR) model and the experimental Texas Tech modeling system (Benjamin et al. 2016; Dowell et al. 2022; James et al. 2022; Ancell 2016) provide only hourly output of these parameters with a horizontal grid spacing of ~ 3 km. Both models also have the ability to output derived products that alert the forecasters to areas of high fire risks (e.g., Lindley et al. 2023).

Recently, the Warn-on-Forecast System (WoFS) has been developed that offers new tools for short-term weather forecasting that are applicable to fire weather applications. WoFS is an ensemble-based rapidly cycling (15 min) analysis and forecast system designed to generate probabilistic forecasts of high-impact weather events (Wheatley et al. 2015; Jones et al. 2016; Skinner et al. 2018; Jones et al. 2020; Heinselman et al. 2024). WoFS generates forecast output at 5-min intervals, which is very important when forecasting rapidly evolving environmental conditions. WoFS has also recently been upgraded with a smoke forecasting capability which allows for some feedback between the forecast smoke and the surrounding environment (Jones et al. 2022, 2024).

2. Red flag threat index

One main challenge for forecasters is determining when conditions are most favorable for wildfire initiation and rapid spread using the constantly increasing number of available forecast products. Parameters have been developed that aggregate environmental forecasts into specific products designed to indicate the favorability of the overall environment for wildfire formation and spread. One such product is the red flag threat index (RFTI), which is a unitless parameter that compares forecast surface humidity and wind speed with a multiyear observed climatology of hourly surface observations to determine when these conditions are most extreme (Murdoch et al. 2012). The primary users of RFTI are both NWS operational forecasts and fire/land management partners in the southern plains (Lindley et al. 2023).

RFTI is generated by first creating an hourly climatology of locally defined red flag fire weather conditions. The thresholds used here for red flag conditions are 6-m wind speed > 20 mph or 6-m wind gust > 35 mph and relative humidity $< 15\%$ which is similar to those used by weather forecast offices (WFOs) in west Texas. However, these thresholds vary significantly depending on WFO and their local climatology. Our initial work only applies a single definition for red flag conditions, but future work will create several climatologies that can be selected by a forecaster for comparison (Kimutis et al. 2018; Jakober et al. 2023). Classic RFTI is derived from ASOS-based climatologies located within an NWS office's coverage area. These ASOS-based climatologies shown here utilize hourly observations over a period of 10–20 years. The site-specific climatologies create somewhat different RFTI thresholds in different areas, which can result in discontinuities of RFTI forecasts from one region to the other. One potential solution to this dilemma is to use a high-resolution reanalysis product to generate the climatological fields. Recently, the Real-Time Mesoscale Analysis (RTMA) product has become available that has the necessary spatial and temporal resolution (3 km, hourly) to generate the climatological fields at the temporal resolution required for RFTI. This new RTMA-based RFTI is labeled the RRFTI with the first "R" indicating the RTMA-based nature of this product. For the RRFTI, the climatology is created from the RTMA at each grid point from January 2019 to 2024. While the potential for creating a continuous climatology for the entire CONUS exists, many regions such as the far northwest and most of the east coast rarely reach the southern plains red flag fire criteria, preventing the initial RRFTI climatology from being created for these regions due to low sample size. Still, the coverage of the RTMA-based climatology greatly exceeds the existing product and can be further expanded by using different red flag criteria. One current disadvantage of the RTMA-based method is that the current RTMA dataset only goes back to 2019, limiting the climatology to 5 years as of this writing.

The humidity and wind speed climatologies are binned by quartiles at each location or grid point, generating minimum, 25th percentile, median, 75th percentile, and maximum thresholds. In the case of the RTMA-based climatology, 1st and 99th percentiles are used as the "minimum" and "maximum" thresholds to remove nonrepresentative extremes in the reanalysis. RFTI and RRFTI are calculated by the sum of two terms related to humidity and wind speed ($RFTI_{RH}$ and $RFTI_{ws}$) both of which are integers ranging from 0 to 5 based on where forecast conditions fall into the climatology thresholds. For both training and application, RTMA and WoFS 10-m winds are converted to 6-m values using an adjustment factor of 0.886. The final RFTI/RRFTI value ranges from 0 to 10 with zero indicating noncritical conditions up to 10, which is considered historic (Table 1).

Substantial spatial variability exists in the RTMA climatologies for all quartiles of relative humidity and wind speed (Fig. 1). The overall coverage is best for western Texas, Oklahoma, and Kansas as well as most of New Mexico, Arizona, Nevada, Colorado, Wyoming, and much of Utah. Other areas along the West Coast do not have enough grid points that satisfy the red flag criteria used here. For relative humidity, quartile values are drier in west Texas, eastern New Mexico, and northern Mexico. Wind quartiles are also elevated in this region but are highest in the plains of eastern Colorado and western Kansas. What this spatial variability indicates is that certain regions require lower relative humidity and higher wind speed values to generate the same RRFTI value than that less dry and windy conditions may generate elsewhere.

TABLE 1. RFTI threshold definitions adapted from Murdoch et al. (2012) and Lindley et al. (2023).

RFTI	Description
1–2	Elevated
3–4	Near critical
5–6	Critical
7–8	Extremely critical
9–10	Historically critical

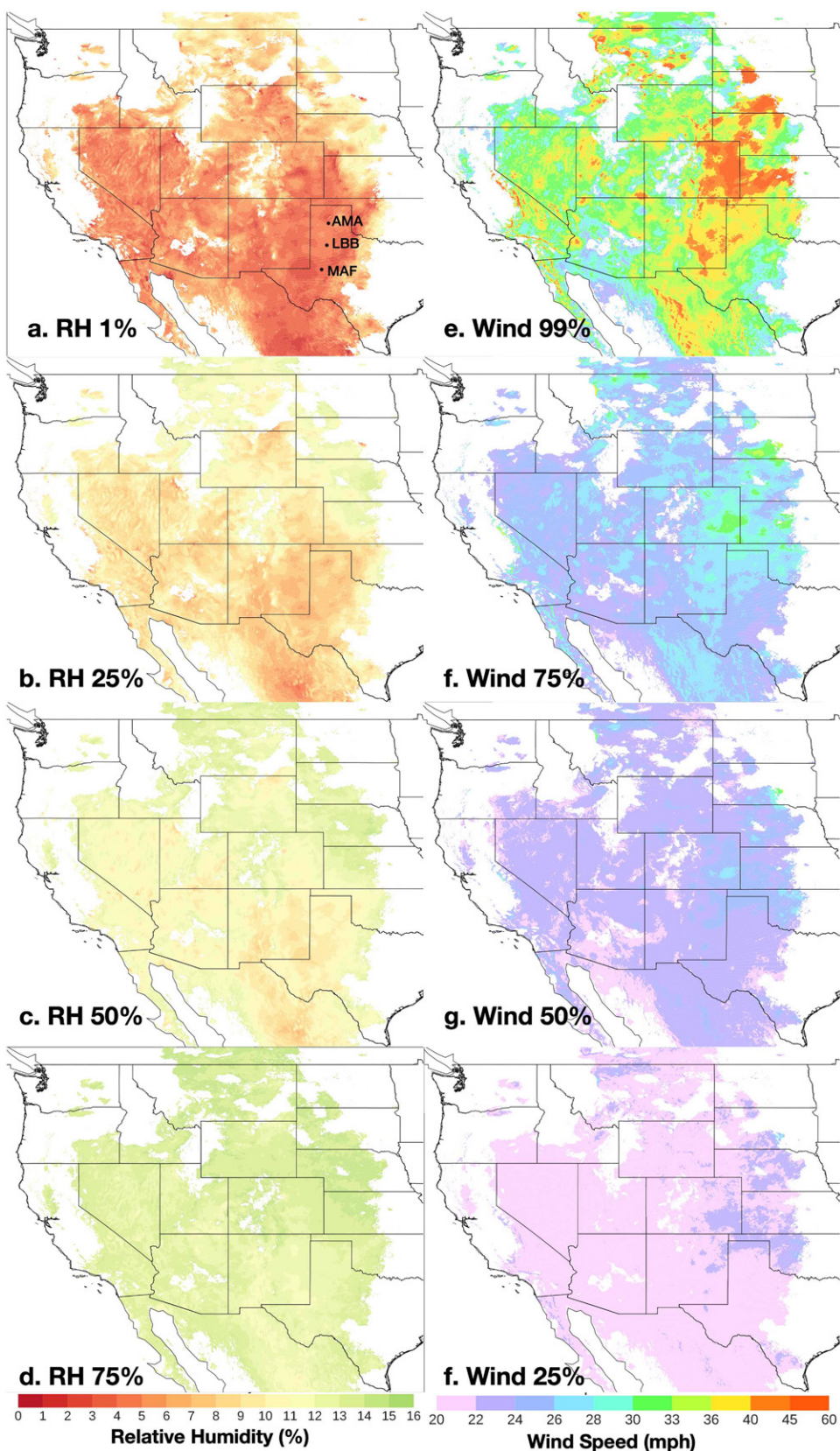


FIG. 1. RTMA-based RH and wind speed climatology quartiles over the W-CONUS. The 99% RH and 1% wind speed values are essentially constant at 15% and 20 mph, respectively. White areas indicate where the sample size of grid points that satisfied the red flag criteria was too small to generate climatological values. Black dots indicate the location of three ASOS sites in western Texas (Amarillo, AMA; Lubbock, LBB; and Midland, MAF) used for verification.

To verify that the 5-yr RTMA-based climatology is generally consistent with specific grid points, we compared the ASOS climatology values at three locations in western TX (Amarillo, Lubbock, and Midland). ASOS climatologies are derived from a ~20-yr sample versus the 5-yr sample of RTMA, so potential climate change factors in the comparison are not taken into account. The resulting ASOS RFTI values were calculated using the most recent available data and differ somewhat from those shown in Murdoch et al. 2012. We also show 1% and 99% percentiles for ASOS data for comparison with the RTMA thresholds instead of the absolute minimum or maximum.

For wind speed, both ASOS- and RTMA-based values are generally within 2 mph of each other for all quartiles and differences for relative humidity are approximately 2% indicating a high degree of agreement (Table 2). One notable difference is that the RTMA-based values are generally drier, which may indicate a bias difference between the observations and reanalysis.

3. Forecast analysis

RRFTI is being incorporated into the WoFS product suite for testing when wildfire risk is high. The first example of evaluating RRFTI occurred on 22 April 2022 following a period of above normal temperatures and below normal precipitation in New Mexico and southern Colorado. Several prescribed burns broke containment leading to high-impact wildfires including the Cooks Peak Fire in northern New Mexico and the Calf Canyon/Hermits Peak Fire farther south, both of which rapidly grew in size on 22 April, with new fires initiating in several other locations further north and east. The Storm Prediction Center (SPC) day 1 fire weather outlook issued at 1639 UTC forecasts a large area of extreme fire weather conditions through most of central and eastern New Mexico up through eastern Colorado (Fig. 2a). The Albuquerque NWS office had also issued a red flag warning for much of the area at 1135 UTC (Fig. 2b). WoFS forecasted these conditions well with 1-, 2-, and 3-h wind gusts and relative humidity forecasts initialized from 2100 UTC showing a very large area of extremely dry air and windy conditions (Fig. 3). The short-term evolution of these conditions is evident in the progression of dry air eastward from New Mexico into western Texas. In western Kansas, the boundary is relatively static, but with a much tighter moisture gradient by 0000 UTC (Figs. 3d–f).

The WoFS 1-h RRFTI forecast valid at 2200 UTC predicts large areas of ensemble mean RFTI > 7 over northern New Mexico and southern Colorado, with smaller, embedded areas of RFTI > 8 indicating extremely critical fire

TABLE 2. Table of wind (mph) and RH (%) quartile values generated from ASOS and RTMA data for three sites located in western Texas (Amarillo, AMA; Lubbock, LBB; and Midland, MAF). RTMA values represent those from the grid point located nearest the ASOS site. Values corresponding to RFTI components 1 and 5 represent 1% and 99% percentiles for both 20-yr ASOS and 5-yr RTMA climatologies.

	RH_{ASOS}	RH_{RTMA}	$Wind_{ASOS}$	$Wind_{RTMA}$
AMA				
1	15.0	15.0	20.0	20.0
2	13.6	12.6	20.2	21.5
3	11.8	9.5	22.3	23.7
4	9.4	7.3	24.3	26.8
5	4.1	4.1	35.4	36.5
LBB				
1	15.0	15.0	20.0	20.0
2	13.6	12.3	20.2	21.8
3	11.8	9.6	22.3	23.4
4	9.5	7.5	25.3	25.9
5	4.3	4.4	36.4	35.5
MAF				
1	15	15	20	20
2	13.4	12.8	20.2	21.2
3	11.5	9.6	22.3	22.9
4	9.1	7.3	24.3	25.2
5	3.7	3.4	33.4	35.6

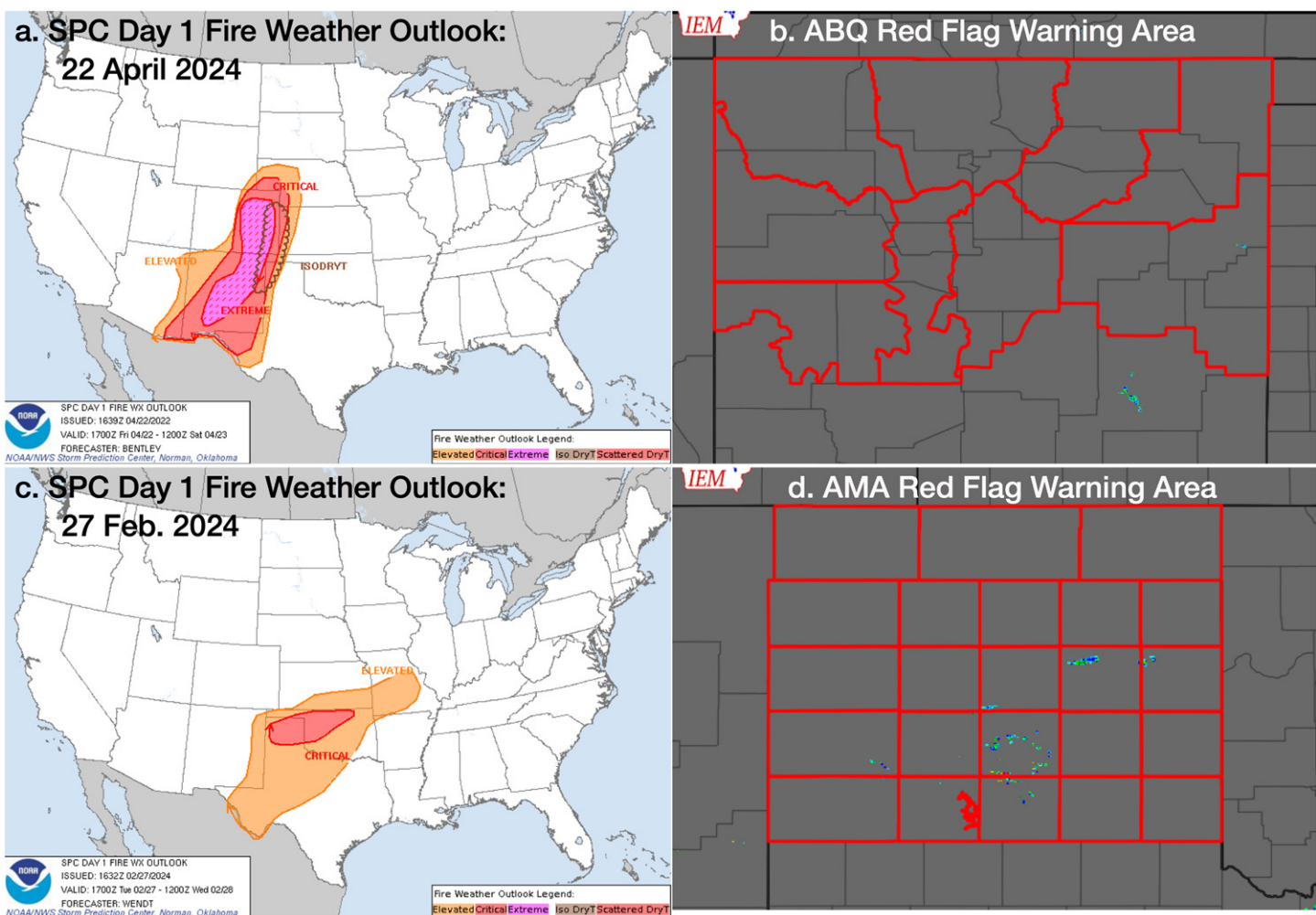


FIG. 2. (a) SPC day 1 fire weather outlook issued at 1639 UTC 22 Apr 2022 highlighting the extreme conditions expected later that day. (b) Red flag warning issued by the Albuquerque NWS office at 1135 UTC highlighting a similar area. (c),(d) Corresponding SPC and NWS (Amarillo) products for 27 Feb 2024 issued at 1632 and 1244 UTC, respectively.

weather conditions (Fig. 4a). The maximum RRFTI values move eastward during the 3-h forecast period, though the magnitude decreases somewhat by 0000 UTC (Figs. 4b,c). This is a result of wind speed decreasing during the evening hours. Recall that WoFS is an ensemble forecasting system, so it is also possible to visualize the probability of RRFTI greater than certain thresholds for a particular forecast time. During this period, the forecast probability of RRFTI exceeding extremely critical conditions (>7) is 100% over much of eastern New Mexico and southern Colorado (Figs. 4d–f). This level of ensemble agreement provides confidence in both the aerial extent and threat level of wildland fire conditions expected to occur in these areas.

The RRFTI product combines the humidity and wind forecasts in this case to highlight areas where extreme fire risk is present that may not be apparent with the humidity or wind speed forecasts alone. The maximum wind speeds are forecast to occur across northern New Mexico and southeastern Colorado, with substantially lower values forecast in eastern New Mexico. However, the extremely low forecast humidity ($<5\%$) throughout this area results in $RFTI_{RH}$ contributing its maximum value of 5 to the total area. The highest RRFTI values then occur where the wind speed forecasts are maximized in the large area of dry air (Figs. 3 and 4). Two major fires located in north-central New Mexico grew significantly larger in these conditions. Additional fires initiated further east corresponding to the movement of favorable conditions during the afternoon. Also note that the smoke plumes grew rapidly to the northeast corresponding to the strong winds present over this area (Figs. 4g–i).

2200 UTC: 1-h forecast

2300 UTC: 2-h forecast

0000 UTC: 3-h forecast

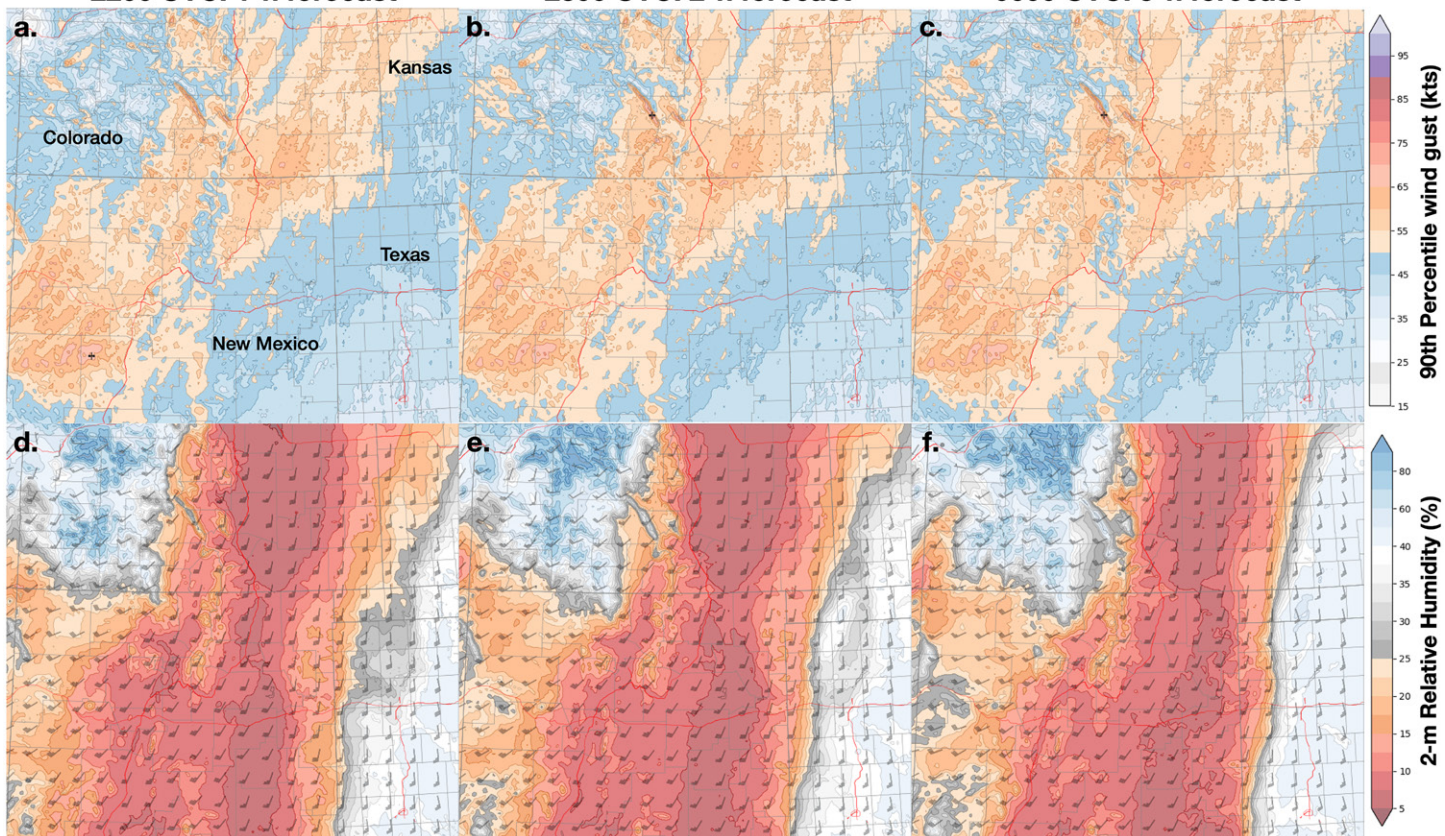


FIG. 3. Forecast surface wind gust and relative humidity conditions from WoFS initiated at 2000 UTC 22 Apr 2022 and shown at 1-, 2-, and 3-h forecast intervals. (a)–(c) Wind gusts are shown as the 90th percentile ensemble value accumulated over the forecast period. (d)–(f) Relative humidity is shown as ensemble mean relative humidity at the lowest model level valid at each forecast time.

Ensemble mean RRFTI forecasts were evaluated retrospectively in the FWT for this case, and the product was found to be very useful in potential forecast situations (Hatchett et al. 2024). Specifically, it was noted that WoFS's ability to forecast rapidly evolving changes in the environment can be very important to determine rapid changes in wildfire risk (increases and decreases) over small areas. The previous version of WoFS was also being run in real time for a severe weather risk in Texas, but the western portion of the domain also happened to domain overlaped with these fires. Lindley et al. (2023) noted that the NWS incident meteorologist assigned to this event used environmental output from WoFS to update forecasters and state forestry agency fire analysts on the short-term evolution of the wildfire threat corresponding to the ignition of new fires along the advancing edge of the favorable conditions.

The largest Texas wildfire on record occurred on 26–27 February 2024, located north and east of Amarillo, Texas. This fire, known as the Smokehouse Creek Fire, burned over one million acres of land. Initial fires were evident on 26 February, and conditions were favorable for their rapid spread on the 27th. The SPC day 1 fire weather outlook issued at 1632 UTC forecasts a large area of elevated fire weather conditions throughout most of western Texas and Oklahoma with an area of critical but not extreme conditions in far northern Texas and northwestern Oklahoma (Fig. 2c). The Amarillo WFO also issued a red flag warning over a similar region in the expectation of dry, windy conditions (Fig. 2d).

Multiple fires were ongoing by mid-day and continued to grow in size and number during the late afternoon. These conditions became more favorable during the afternoon due to both decreases in relative humidity and increases in wind speed (Fig. 5). An increase in RRFTI from 3–4 to 6–7 in Texas during the 3-h forecast period initiated at 1900 UTC corresponds

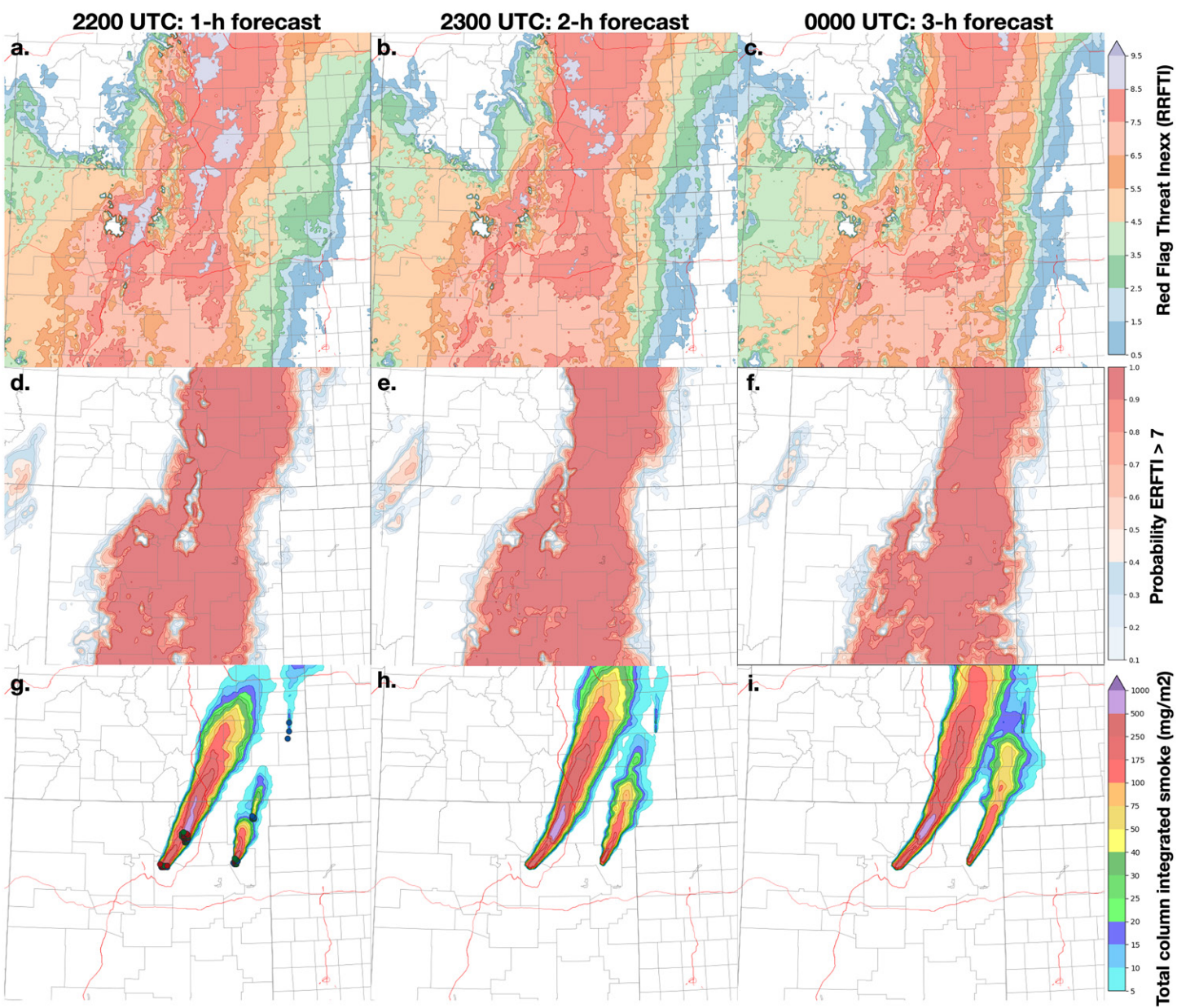


FIG. 4. (a)–(f) Ensemble mean RRFTI and probability of RRFTI > 7 forecasts from WoFS initiated at 2000 UTC 22 Apr 2022 and shown at 1-, 2-, and 3-h forecast intervals. (g)–(i) Ensemble mean total integrated smoke forecast with GOES-16 FRP retrieval from 2000 UTC overlaid.

to the changing conditions (Figs. 6a–c). The probability of RRFTI > 5 shows that the highest confidence of these conditions is present over the Oklahoma Panhandle, with other areas in western Texas, and eastern New Mexico at 2000 UTC (Figs. 6d–f). At later forecast times, the probability of critical conditions increases over much of west Texas. By 2200 UTC, large areas of $>80\%$ probabilities are forecast near where the large wildfires would occur (Fig. 6f). Note that the threshold of 7 used for the 22 April case was not used here as that value was rarely exceeded on this day resulting in very low probabilities of extremely critical conditions (not shown). Classic RFTI values calculated at the West Texas Mesonet sites of Stinnett and Canadian were also consistently at 5 or above after 2000 UTC (Fig. 7). RFTI at these sites reached 6 between ~ 2100 and ~ 2145 UTC, which is consistent with the forecast increase in RRFTI after 2000 UTC. Classic RFTI values rarely reach or exceed 7 at these sites.

This increase in RRFTI corresponded to a rapid increase in the number and size of the fires. By 1900 UTC, over 150 fire pixels were retrieved from GOES-16 imagery at each scan time within this domain. Also present during this event was a southward moving cold front,

2000 UTC: 1-h forecast

2100 UTC: 2-h forecast

2200 UTC: 3-h forecast

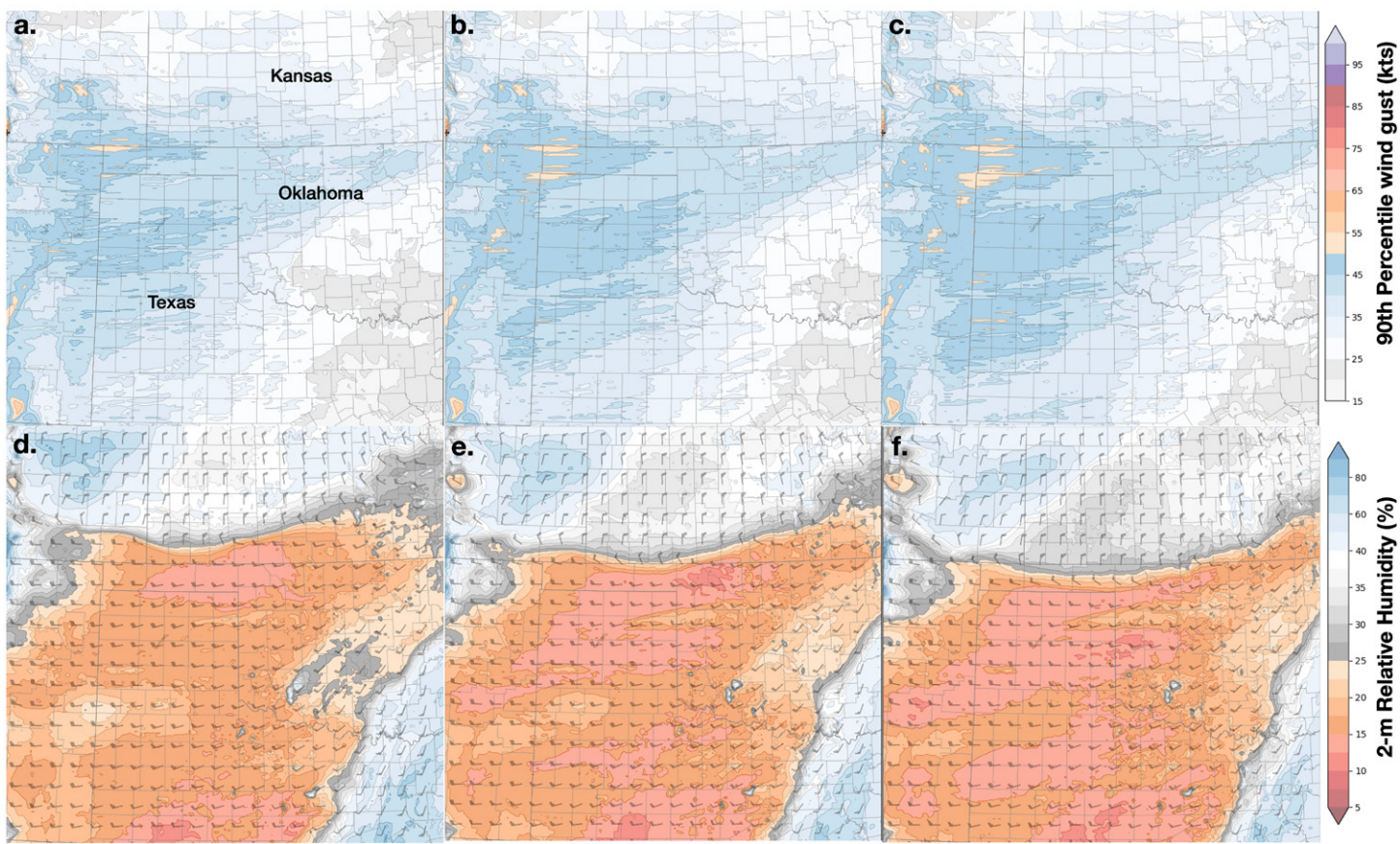


FIG. 5. As in Fig. 3, but for 27 Feb 2024 with WoFS forecasts initiated at 1900 UTC.

whose boundary is evident from the very tight relative humidity gradient. The front would begin to interact with these fires by 2300 UTC, which was 1–2 h quicker than forecast by early WoFS initiation times and other CAMS. Large smoke plumes emanating from these fires were also forecast extending far eastward into much of Oklahoma by 2200 UTC (Figs. 6g–i). One impact of smoke being present in the system is the thermodynamic coupling between smoke aerosols and the environment. Thus, the surface under the smoke plume is cooled relative to the smoke free areas, generating a localized increase in relative humidity. This results in a localized decrease in RFTI relative to the surrounding environment, where the smoke plumes are present.

Comparing this event to the New Mexico fires shows that a specific RRFTI threshold does not necessarily correspond to the size and impact of a fire. Conditions in New Mexico on 22 April 2022 were extremely favorable for wildfire spread, and those fires did indeed occur. Environmental conditions present in Texas on 27 February 2024 did not appear as extreme but still exceeded the criteria for high impact fires. The Smokehouse Creek Fire also occurred under very favorable fuel conditions that included large areas of dry grass within the Canadian River Valley, which contains terrain features known to enhance southwesterly winds. The rapid change in wind direction from westerly to due northerly occurring around 2300 UTC during passage of the cold front also allowed the fire to access unburned fuels not in the original path. Poor forecasts of frontal passage during wildfire events have also been noted in Lindley et al. (2006). All these conditions combined represent an extreme threat for wildfire spread also indicating the need of parameters beyond atmospheric conditions in future threat indices.

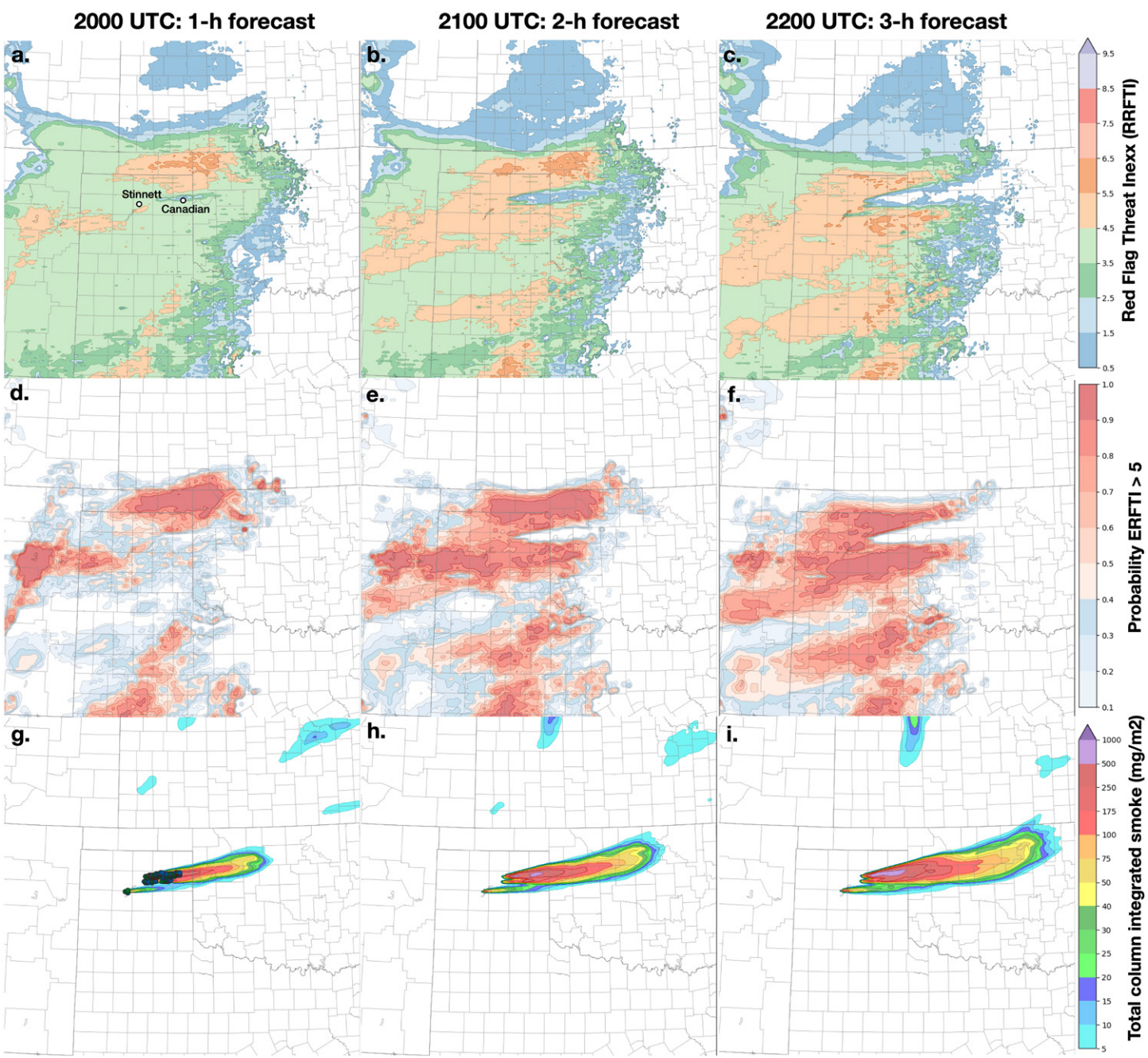


FIG. 6. As in Fig. 4, but for 27 Feb 2024 with WoFS forecasts initiated at 1900 UTC and probability of RRFTI > 5 instead of 7. Locations of the Stinnett and Canadian West Texas Mesonet sites are overlaid.

4. Discussion

Further development of RRFTI is ongoing based on continued forecast evaluation with an emphasis on extending use of both the index and CAMs in fire meteorology, as well as incorporating surface conditions such as soil moisture into this index. Work is underway to generate “high,” “medium,” and “low” red flag environment climatologies to better capture the range of red flag criteria used by various WFOs. The high climatology will utilize high wind speed and low RH thresholds while medium and low climatologies will relax these criteria in regions where the extremely dry and windy conditions are less common. The medium and low criteria will also result in larger geographic coverage for RRFTI. In operations, a forecaster will be able to select the climatology field most suited to the local conditions and plot the corresponding RRFTI value that fits those conditions. This parameter would also be useful in regions where legacy RH and wind speed climatologies do not exist. In addition, we expect

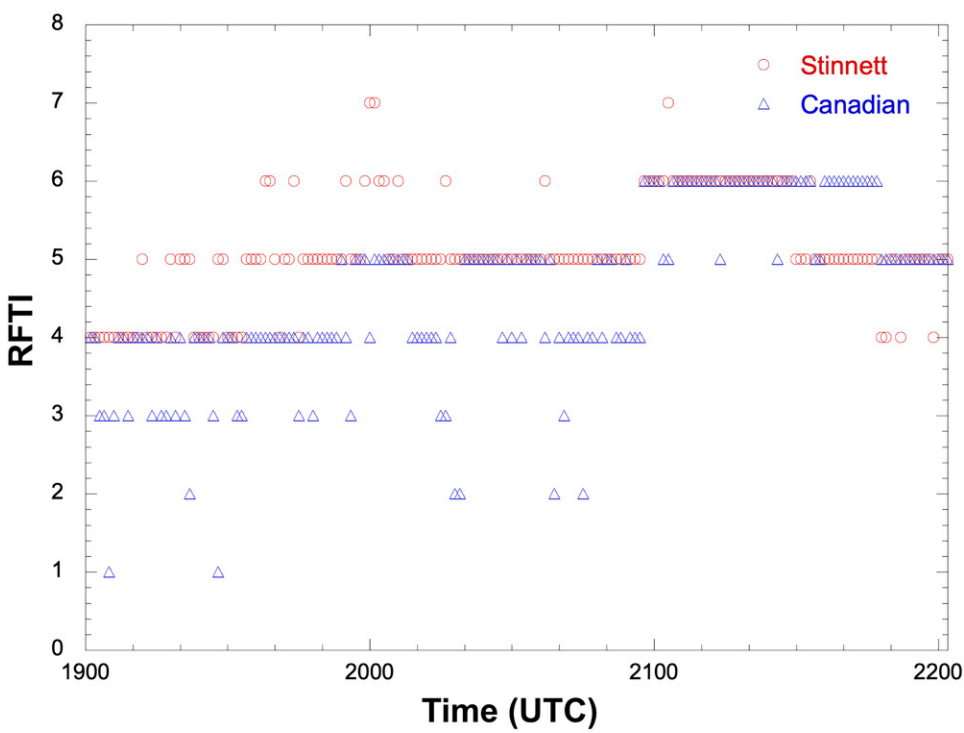


FIG. 7. Classic RFTI calculated at 1-min intervals from West Texas Mesonet data located at Canadian and Stinnett between 1900 and 2200 UTC.

to include fuel information such as the NFDRS energy release component product as part of the process, which is already being used with the classic RFTI in operations (Jakober et al. 2023; Lindley et al. 2024). Finally, future versions of WoFS will operate at higher density grid spacings, allowing for very fine-scale changes in environmental conditions to be taken into account for fire weather forecasts.

Acknowledgments. This research was funded in part by the NOAA Warn-on-Forecast project. Additional funding was provided under the NOAA-University of Oklahoma Cooperative Agreement NA21OAR4320204, U.S. Department of Commerce.

Data availability statement. All forecast output described in research are available online at <https://wof.nssl.noaa.gov/wofs-smoke>. RTMA data used to create the climatology fields are available at <https://aws.amazon.com/>.

References

Ancell, B. C., 2016: Improving high-impact forecasts through sensitivity-based ensemble subsets: Demonstration and initial tests. *Wea. Forecasting*, **31**, 1019–1036, <https://doi.org/10.1175/WAF-D-15-0121.1>.

Benjamin, S. G., and Coauthors, 2016: A North American hourly assimilation and model forecast cycle: The Rapid Refresh. *Mon. Wea. Rev.*, **144**, 1669–1694, <https://doi.org/10.1175/MWR-D-15-0242.1>.

Chow, F. K., and Coauthors, 2022: High-resolution smoke forecasting for the 2018 Camp Fire in California. *Bull. Amer. Meteor. Soc.*, **103**, E1531–E1552, <https://doi.org/10.1175/BAMS-D-20-0329.1>.

Dowell, D. C., and Coauthors, 2022: The High-Resolution Rapid Refresh (HRRR): An hourly updating convection-allowing forecast model. Part I: Motivation and system description. *Wea. Forecasting*, **37**, 1371–1395, <https://doi.org/10.1175/WAF-D-21-0151.1>.

Hatchett, B. J., J. L. Vickery, Z. T. Tolby, T. A. Jones, P. S. Skinner, E. M. Wells, and K. J. Thiem, 2024: Fire Weather Testbed Evaluation #001: The Warn-On-Forecast smoke system. NOAA Tech. Memo. OAR GSL-68, 50 pp., <https://doi.org/10.25923/nd0m-4j95>.

Heinselman, P. L., and Coauthors, 2024: Warn-on-Forecast System: From vision to reality. *Wea. Forecasting*, **39**, 75–95, <https://doi.org/10.1175/WAF-D-23-0147.1>.

Jakober, S., T. Brown, and T. Wall, 2023: Development of a decision matrix for National Weather Service red flag warnings. *Fire*, **6**, 168, <https://doi.org/10.3390/fire6040168>.

James, E. P., and Coauthors, 2022: The High-Resolution Rapid Refresh (HRRR): An hourly updating convection-allowing forecast model. Part II: Forecast performance. *Wea. Forecasting*, **37**, 1397–1417, <https://doi.org/10.1175/WAF-D-21-0130.1>.

Jones, T., R. Ahmadov, E. James, G. Pereira, S. Freitas, and G. Grell, 2022: Prototype of a Warn-on-Forecast System for Smoke (WoFS-Smoke). *Wea. Forecasting*, **37**, 1191–1209, <https://doi.org/10.1175/WAF-D-21-0143.1>.

—, —, —, —, —, and —, 2024: Ingesting GOES-16 fire radiative power retrievals into WoFS-Smoke. *Int. J. Wildland Fire*, **33**, WF23133, <https://doi.org/10.1071/WF23133>.

Jones, T. A., K. Knopfmeier, D. Wheatley, G. Creager, P. Minnis, and R. Palikonda, 2016: Storm-scale data assimilation and ensemble forecasting with the NSSL Experimental Warn-on-Forecast System. Part II: Combined radar and satellite data experiments. *Wea. Forecasting*, **31**, 297–327, <https://doi.org/10.1175/WAF-D-15-0107.1>.

—, and Coauthors, 2020: Assimilation of GOES-16 radiances and retrievals into the Warn-on-Forecast System. *Mon. Wea. Rev.*, **148**, 1829–1859, <https://doi.org/10.1175/MWR-D-19-0379.1>.

Kimutis, N., T. Wall, and T. Brown, 2018: Red flag warning and fire weather watch issuance criteria. Fall Colloquium, Community College Undergraduate Research Initiative, 2 pp., https://www.researchgate.net/profile/Nicholas-Kimutis/publication/329352281_Red_Flag_Warning_Fire_Weather_Watch_Issuance_Criteria/links/5c02fbe245851523d1569bbe/Red-Flag-Warning-Fire-Weather-Watch-Issuance-Criteria.pdf.

Lindley, T. T., M. Conder, J. Cupo, C. Lindsey, G. Murdoch, and J. L. Guyer, 2006: Operational implications of model predicted low-level moisture and winds prior to the New Year's Day 2006 wildfire outbreak in the Southern Plains. *Electron. J. Oper. Meteor.*, **2006-EJ7**, <http://nwafiles.nwas.org/ej/pdf/2006-EJ7.pdf>.

—, A. B. Zwink, R. R. Barnes, G. P. Murdoch, B. C. Ancell, P. C. Burke, and P. S. Skinner, 2023: Preliminary use of convection-allowing models in fire weather. *J. Oper. Meteor.*, **11**, 72–81, <https://doi.org/10.15191/nwajom.2023.1106>.

—, and Coauthors, 2024: Retrospective demonstrations of an integrated team approach to fire warnings for western United States wildfire disasters. *J. Oper. Meteor.*, **12**, 54–71, <https://doi.org/10.15191/nwajom.2024.1205>.

Murdoch, G. P., R. R. Barnes, C. M. Gitro, T. T. Lindley, and J. D. Vitale, 2012: Assessing critical fire weather conditions using a Red Flag Threat Index. *Electron. J. Oper. Meteor.*, **13**, 46–56, <http://nwafiles.nwas.org/ej/pdf/2012-EJ4.pdf>.

Parks, S. A., M.-A. Parisien, C. Miller, and S. Z. Dobrowski, 2014: Fire activity and severity in the western US vary along proxy gradients representing fuel amount and fuel moisture. *PLOS ONE*, **9**, e99699, <https://doi.org/10.1371/journal.pone.0099699>.

Peace, M., J. Charney, and J. Bally, 2020: Lessons learned from coupled fire-atmosphere research and implications for operational fire prediction and meteorological products provided by the Bureau of Meteorology to Australian Fire Agencies. *Atmosphere*, **11**, 1380, <https://doi.org/10.3390/atmos11121380>.

Skinner, P. S., and Coauthors, 2018: Object-based verification of a prototype Warn-on-Forecast System. *Wea. Forecasting*, **33**, 1225–1250, <https://doi.org/10.1175/WAF-D-18-0020.1>.

Troy, A., J. Moghaddas, D. Schmidt, J. S. Romsos, D. B. Sapsis, W. Brewer, and T. Moody, 2022: An analysis of factors influencing structure loss resulting from the 2018 Camp Fire. *Int. J. Wildland Fire*, **31**, 586–598, <https://doi.org/10.1071/WF21176>.

Wheatley, D. M., K. H. Knopfmeier, T. A. Jones, and G. J. Creager, 2015: Storm-scale data assimilation and ensemble forecasting with the NSSL Experimental Warn-on-Forecast System. Part I: Radar data experiments. *Wea. Forecasting*, **30**, 1795–1817, <https://doi.org/10.1175/WAF-D-15-0043.1>.